DOI: 10.18721/JPM.10202
UDC 543.084.852; 351.814.375.3

SPECIAL FEATURES OF RADIO CONTROL LINK FOR ENERGY EFFICIENT LED LIGHT SOURCES

A.V. Aladov[1], V.P. Valyukhov[2], V.D. Kuptsov[2], S.V. Demin[1], A.V. Valyukhova[2]

[1]Submicron Heterostructures for Microelectronics Research and Engineering Center of the RAS, St. Petersburg, Russian Federation

[2]Peter the Great St. Petersburg Polytechnic University, St. Petersburg, Russian Federation

The aim of the study is to reveal the special features of radio control link model in LR-WPAN under operating conditions of interference of the reflected and the line-of-sight component and to evaluate the radio link's range of positive light source control. The results of development and practical implementation of controlled spectrally tunable light emitting diode (LED) light sources with ISM- and ZigBee(IEEE 802.15.04)-based radio frequency transceivers are presented. A software application developed in LabVIEW simulation of a radio control link for light sources and used for evaluating the radio control link's range of various combinations of polarization of transmitting and receiving antennas has been discussed. It was established and experimentally verified that the received energy was able to be computed using the two-ray model: a line-of-sight ray and the reflected one. This approach is simpler as compared to cellular networks in which multiple reflections from various objects result in multi-path propagation without line-of-sight component.

Key words: controlled light source; interference; technology; led; link control range; antenna

Citation: A.V. Aladov, V.P. Valyukhov, V.D. Kuptsov, S.V. Demin, A.V. Valyukhova, Special features of radio control link for energy efficient LED light sources, St. Petersburg Polytechnical State University Journal. Physics And Mathematics. 10(2) (2017) 16–27. DOI: 10.18721/JPM.10202

ОСОБЕННОСТИ РАДИОКАНАЛА УПРАВЛЕНИЯ ЭНЕРГОЭФФЕКТИВНЫМИ СВЕТОДИОДНЫМИ ИСТОЧНИКАМИ ОСВЕЩЕНИЯ

А.В. Аладов[1], В.П. Валюхов[2], В.Д. Купцов[2], С.В. Демин[1], А.В. Валюхова[2]

[1]Научно-технологический центр микроэлектроники и субмикронных гетероструктур РАН, Санкт-Петербург, Российская Федерация

[2]Санкт-Петербургский политехнический университет Петра Великого, Санкт-Петербург, Российская Федерация

Исследована модель радиоканала управления беспроводной сети LR-WPAN в условиях интерференции прямой и отраженной волн, а также изучена достижимая дальность безотказного управления светодиодными источниками освещения по радиоканалу. Приведены результаты разработки и практической реализации управляемых, спектрально перестраиваемых светодиодных источников освещения, радиочастотные трансиверы которых выполнены по технологиям ISM (868 МГц) и ZigBee (IEEE 802.15.04, 2445 МГц). Рассмотрена LabVIEW-версия моделирования радиолинии управления источниками освещения с учетом особенностей их практического применения для определения диапазона

по дальности при различных комбинациях ориентации (поляризации) антенн передатчика и приемника.

Ключевые слова: управляемый источник освещения; интерференция; светодиод; диапазон по дальности; антенна; передатчик; приемник

Ссылка при цитировании: Aladov A.V., Valyukhov V.P., Kuptsov V.D., Demin S.V., Valyukhova A.V. Special features of radio control link for energy efficient LED light sources // St. Petersburg Polytechnical State University Journal. Physics and Mathematics. 2017. Vol. 10. No. 2. Pp. 16–27. DOI: 10.18721/JPM.10202

Introduction

According to the research results on the effects of indoor lighting environments on human organism, poor illumination or color temperature of lighting sources can affect users' vision and divide their attention, and hence, cause users to feel tired or fretful [1, 2]. Light emitting diodes (LEDs) satisfy the requirements to modern light sources, first of all, because their high energy efficiency, luminous efficacy of 150 lm/W in mass-produced LEDs, allows sufficient savings in energy consumption. Also the ability to improve the quality of generated light by dynamic control of spectral-color parameters (smart light based on RGB-mixing). The quality of generated light depends, first of all, on the ability to produce light with a wide range of color temperatures (2700 – 6500 K) with high color rendering indexes [3].

This paper presents the results of theoretical studies of achievable radio control link's range in Low Rate-Wireless Personal Area Network (LR-WPAN) and practical implementation of wireless networks of energy-efficient dynamically controlled LED light sources using ISM (868 MHz) and ZigBee (IEEE 802.15.04, 2445 MHz) technologies.

The LED sources are used for illumination of living, communal and industrial quarters with the ability to regulate color, spectral and brightness lighting characteristics with time and the creation of an optimal lighting environment. The LED light sources described below produce white light with the required spectral, color and brightness characteristics using the principle of RGBW color-mixing: controlled polychromatic LED light source (CPLLS) and energy-efficient dynamically controlled LED light sources (EDCLLS).

Most European wireless equipment operates at 2.4 GHz, however, 868 MHz is used for some narrow band and wide band applications, such as street light control, social alarm, generic alarm and non-specific small range distances (SRDs) systems.

ZigBee is a standard based on the IEEE 802.15.4 standard for wireless personal networks. This standard allows for the creation of very lost cost and low power networks. These networks are created from sensors and actuators and can wireless control many electrical products such as remote controls, medical, industrial, and security sensors [4].

Practical implementation of CPLLS and EDCLLS networks

The wireless CPLLS and EDCLLS networks contain the following components: terminal devices (lamps) with LED light sources playing their role; a remote control station (RCS), which coordinates the network and controls its operation in all modes; a PC that also serves as a network coordinator when setting up the network and for some modes of its operation. The CPLLS and EDCLLS devices themselves include the following components: a power supply for standby mode; a main power supply; a microcontroller with a control board including a wireless link; LED drivers for power management; LED bars with series-connected LEDs.

The SPLLS and EDCLLS which form a LR-WPAN are intended for use in good-sized rooms in all three dimensions (length, width, height). This influences the radio control link analysis. The orientation of the transmitting and receiving antennas with respect to the ground may result in a complex configuration that must be taken into account when designing light sources. Light sources are controlled using a remote control station. Hand-held equipment is generally operated close to the ground and this implies that the ground influence has to be considered to do valid range calculations for the link.

It is assumed that the path has a line-of-sight (LoS) component that is limited by free-

space loss (large open room, large retail stores, sports arenas, open-plan offices, exhibition halls), but not by additional loss due to obstacles and transmission through building materials, and there is no mitigation of free-space loss by channeling.

The CPLLS's color temperature lies in the range between 2700 and 6500 K, the light intensity does in the range between 1700 and 2400 lm, and this network exhibits high values of color rendering indexes (no less than 80 – 90). The power used by the source is less than 20 W (18.4 W), luminous efficacy is 85 – 120 lm/W. Six drivers transform the constant current from a power supply to the LED's feed current with pulse width modulation (PWM). Total supply current is no more than 1 A. The PWM frequency was set by a microcontroller within a range of 1.25 – 10 kHz and the duty cycle of PWM varied from 100 (1% PWM) to 1 (100% PWM). The brightness was varied by increasing the PWM period relative to the brightness at the optimal PWM frequency (F_{opt} = 2.5 kHz), corresponding to 100% light intensity of the LED unit. At 10% light intensity the PWM period corresponds to 250 kHz frequency. This improves the speed of CPLLS and is higher than the 100 Hz threshold sensitivity of a human eye to the modulation of brightness. RCS operating in the 868.7 – 869.2 MHz band can be used with narrow or wide band (NB and WB, respectively) modulations, has the transmitter effective radiated power (ERP) 25 mW (+14 dBm) and duty cycle less than 0.1 %. The receiver category is defined by ETSI EN 300-220-1. A microcontroller receives commands from an RF transceiver using the SPI interface, controls the current drivers for LEDs, and turns the light source on and off. The same transceiver chip CC1110FX is used in the microcontroller board and in the RCS. The chip is a low-power SoC (System-on-Chip) ISM/SRD with MCU, Memory, USB controller and high sensitivity (–110 dBm at 1.2 kBaud and –87 dBm at 250 kBaud). Receiver has high selectivity and good blocking performance, programmable data rate up to 500 kBaud and output power up to 10 dBm, low current consumption (RX: 16.2 mA @ 1.2 kBaud, TX: 15.2 mA @ – 6.0 dBm). There are two power-saving modes: Power Mode 1 (0.8 μA) and Power Mode 2 (0.6 μA). The CC1110FX uses the GFSK (Gaussian Frequency – Shift Keying) modulation.

The CC1110 chip is compatible with many PCB mounted antennas including a DN024 antenna that is used in a RCS and microcontroller unit as a transmitting and a receiving antenna respectively. An RCS controls CPLLS according to the program entered by the operator manually after pressing the 'ON' button and setting the color temperature using the light intensity control button. In the standby mode the CPLLS power consumption is less than 0.5 W.

The CPLLS network has a star topology. The RCS serves as the network coordinator, and the light sources do terminal devices.

Circuit design and technical specification of the RF channels of a RCS and the control microcontroller of EDCLLS are identical because the same module – ZigBit 2.4 GHz Single chip Wireless Module ATZB-S1-256-3-0-C [5] supporting IEEE 802.15.4 standard is used. The module has high sensitivity (–97 dB at error rate BER 1%) and optimal transmitter output power of +3 dBm result in unique power budget (up to 100.6 dB) of the link. The range of the radio control link in free space if the transceivers are positioned at the height of 0.5 m above ground is 170 – 570 m. This is achieved for various combinations of the transceivers' orientations (polarizations) and in the absence of interference from other transmitters. In real life situations the multi-path propagation, the interference and other factors can significantly reduce the range of the radio control link.

Model of radio control link

The idealized model of a radio control link is often described by the Friis transmission equation [6]:

$$P_R = P_T \frac{G_T G_R \lambda^2}{(4\pi)^2 d^n} \qquad (1)$$

where P_R is a power available at the receiving antenna; P_T is a power supplied to the transmitting antenna; G_R, G_T are the gains of the receiving and the transmitting antennas, respectively; λ is the wavelength ($\lambda = c / f$, c is the light speed in vacuum, f is the frequency), d is the distance between two antennas (the

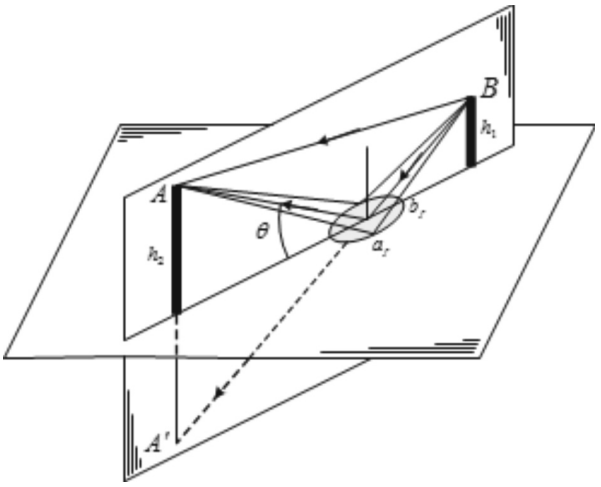

Fig. 1. Two-ray interference scheme of radio control link.
The horizontal plane is an infinite, perfectly flat ground one; points *A* and *B* show the positions of the transmitting and the receiving antennas; the rays' directions are shown by arrows

projection on the Earth's surface), *n* is the path loss exponent.

Eq. (1) is often used to determine the power budget of a radio control link. In real control links the waves are reflected and obstructed by all objects illuminated by the transmitting antenna. In this paper, a two-ray interference model is used where the ground reflecting incident wave toward the transmitting antenna influences the radiation pattern. The interference of the two rays at a receiving antenna produces a particular multi-lobe field structure.

Fig. 1 represents schematically the position where there is an infinite, perfectly flat ground plane and there are no other objects obstructing the signal path.

The refracted wave, describing the penetration of the energy into the soil through the reflecting interface, is usually not taken into account due to high absorption of high-frequency radio waves.

Points *A* and *B* show the positions of the transmitting and the receiving antennas. The field at the receiving antenna is a sum of the direct ray and the ray reflected from the ground (secondary wave). The paths of the rays are R_1 and R_2, respectively, the length of the control link $R = d$, the heights of the transmitting and receiving antennas are h_1 and h_2, it is assumed that $h_1 > \lambda$ and $h_2 > \lambda$. The effect of the reflected ray can be imitated by a fictional source located under the Earth's surface symmetrically to the real source.

In sufficiently long control links $R >> h_1, h_2$ and the rays AB and $A'B$ can be assumed to be parallel, the difference in distance travelled by the rays $R_2 - R_1$ is

$$\Delta R = R - R_1 = 2h_1 \sin\theta$$

that is much smaller than *R*, and it is possible to assume

$$1/R_1 \approx 1/R_2 \approx 1/R$$

and in the calculations of the amplitudes of the direct and the reflected rays.

With these assumptions the interference formula describing the power at the receiving antenna is given by

$$P_R = P_T \frac{G_T G_R \lambda^2 |V|^2}{(4\pi R)^2} \qquad (2)$$

where $|V|$ is the ground influence factor depending on the heights of the antennas above the ground, the reflectivity of the ground and the antennas' radiation pattern.

Other factors are the same as in the Friis transmission equation. The reflected ray is formed by an area of the ground's surface that is determined by the first Fresnel's zone. The Fresnel's zone is shaped like an ellipse with the long axis oriented in the direction of the wave propagation. The lengths of the short and the long axes (see Fig. 1) are, respectively

$$b_f = \sqrt{\frac{h_1 h_2}{(h_1 + h_2)\sin\theta}},\ a_f = \frac{b_f}{\sin\theta}. \qquad (3)$$

The assumption of the direct and reflected rays being parallel needs additional clarification in the case of RSD radio control links. In actuality,

$$R_2^2 - R_1^2 = 4h_1 R_1 \sin\theta - 4h_1^2.$$

Assuming $(R_1 + R_2) \approx 2R$, the difference in distances travelled is

$$\Delta R = R_2 - R_1 = 2h_1 \sin\theta - 2h_1/R.$$

The discrepancy in ΔR between the approximate and real cases is $2h_1/R$ and can be neglected if it is much smaller than π.

The concept of parallel rays is applicable if

$$2kh_1^2/R << \pi \text{ or } R >> 4h_1^2/\lambda.$$

Both SPLLS and EDCLLS are used in combination with a remote control station (RCS). In the former case the RCS is controlled by a human operator. This limits the transmission antenna height to 1.5 – 1.8 m. In the latter case the RCS automatically changes parameters with time without the attention of a human operator. The height of the receiving antenna may reach 2.4 m (standard ceiling height in a modern building). It follows from Fig. 1 that the tangent of the incidence angle θ is

$$\text{tg}\theta = \frac{h_1 + h_2}{d}. \quad (4)$$

The amplitudes of the reflected wave E_R and the direct wave E_T depend on the distance difference $(R_2 - R_1)$ where

$$R_1 = \sqrt{d^2 + (h_1 - h_2)^2},\ R_2 = \sqrt{d^2 + (h_1 + h_2)^2}. \quad (5)$$

In the maximum points the function

$$\cos k(R_2 - R_1) = -1,$$
$$(R_2 - R_1) = (2n_f - 1)\lambda/2,$$

the distances to the maximums of the radiation pattern are equal to

$$R_{\max} = \left[\frac{16h_1^2h_2^2}{(2n_f - 1)^2\lambda^2} - (h_1^2 + h_2^2) + \frac{(2n_f - 1)^2\lambda^2}{16}\right]^{\frac{1}{2}}. \quad (6)$$

In the minimum points the function

$$\cos k(R_2 - R_1) = +1,$$
$$(R_2 - R_1) = n_f\lambda,$$

the distances to the minima of the radiation pattern are equal to

$$R_{\min} = \left[\frac{4h_1^2h_2^2}{n_f^2\lambda^2} - (h_1^2 + h_2^2) + \frac{n_f^2\lambda^2}{4}\right]^{\frac{1}{2}}. \quad (7)$$

In the case of $h_1 \approx h_2$, the following equations for the coordinates of the maxima and minima are used:

$$R_{\max} = \frac{4h_1h_2}{(2n_f - 1)\lambda} - \frac{(2n_f - 1)\lambda}{4},$$
$$R_{\min} = \frac{2h_1h_2}{n_f\lambda} - \frac{n_f\lambda}{2} \quad (8)$$

where n_f = 1, 2, ... is the Fresnel's zone number.

The calculation data obtained for radiation patterns of SPLLS and EDCLLS light sources are presented in Table 1. In addition to this data we obtained the value $2kh_1/R_1 = 2.06$, $R >> 26$ m for SPLLS light source and for $h_1 = 1.5$ m. Then, $2kh_1/R_1 = 0.96$, $R >> 73.34$ m for EDCLLS light source, for $h_1 = 1.5$ m and $h_2 = 6.5$ m. In this case the concept of parallel rays is inapplicable in many practical applications.

The relative amplitude of the reflected wave is described by reflection coefficients known in optics as Fresnel's coefficients. In the cases of horizontal, vertical and circular polarizations

Table 1

Calculation data for radiation patterns of two light sources

h_1, m	$R_{\min 1}$, m		$R_{\max 1}$, m		$\theta_{\min 1}$, D		$\theta_{\max 1}$, D	
	SPLLS	EDCLLS	SPLLS	EDCLLS	SPLLS	EDCLLS	SPLLS	EDCLLS
1.5	56.42	158.92	112.84	317.84	7.58	2.52	4.00	1.08
2.4	90.27	254.27	180.55	553.68	5.09	1.43	4.18	0.34

Notes. 1. The performance data of the light sources are the following: f = 868.7 MHz, λ = 0.3456 m (SPLLS) and f = 2445 MHz, λ = 0.1227 m (EDCLLS).
2. h_1 is the transmitting antenna height, the receiving antenna heights are the same for the both light sources (h_2 = 6.5 m).
Symbols: $R_{\min 1}$, $R_{\max 1}$ are the minimum and the maximum of the first Fresnel's zone of the radiation pattern, θ are the incident angles.

they are given by

$$\Gamma_h = \frac{\sin\theta - \sqrt{\eta - \cos^2\theta}}{\sin\theta + \sqrt{\eta - \cos^2\theta}},$$
$$\Gamma_v = \frac{\eta\sin\theta - \sqrt{\eta - \cos^2\theta}}{\eta\sin\theta + \sqrt{\eta - \cos^2\theta}}, \qquad (9)$$
$$\Gamma_c = \frac{\Gamma_h + \Gamma_v}{2},$$
$$\eta = \varepsilon_r - j60\sigma\lambda$$

where Γ_h, Γ_v, Γ_c are the horizontal, vertical and circular polarization reflection coefficients, respectively; ε_r, σ and η are the permittivity, the conductivity and the complex permittivity of the reflecting medium.

The reflection coefficients are complex numbers meaning that during reflection not only the amplitude of the reflected wave changes but also its phase does. Assuming that both media have equal permeability $\mu_r = 1$ and that one medium is a free space, the reflection coefficient depends only on the complex permittivity of the material. The complex permittivity of typical building materials, obtained experimentally [7], demonstrates significant variations from one material to another, while showing a little frequency dependence (see Table 2).

The presence of the imaginary part of the complex electric permittivity is an evidence of the presence of the electrical conductance. However, numerical estimation show that the influence of the imaginary part of η can be neglected during calculations of the coefficients Γ_h and Γ_v.

At a frequency of 2445 MHz, the minimum of the first Fresnel's zone $R_{\min 1} = 58.68$ m, the incidence angle $\theta = 3.8°$, the reflection coefficients $\Gamma_h = -0.834 + j0.024$, $\Gamma_v = -0.762 - -j0.005$ for $h_1 = 1.5$ m, $h_2 = 2.4$ m, $\eta = 2.0 - j0.5$. Assuming $\eta = 2$, the reflection coefficients are $\Gamma_h = -0.876$, $\Gamma_v = -0.767$, thus the assumption of $\sigma = 0$ does not produce significant errors.

To calculate the range of a radio control link let us use the model [6] that accounts for the ground reflection. The same paper presents the experimental results validating the ground reflection model. The necessary formulae are the following:

$$\theta = \arctan\frac{h_1 + h_2}{d},$$
$$R_1 = \sqrt{d^2 + (h_1 - h_2)^2}, \quad R_2 = \sqrt{d^2 + (h_1 + h_2)^2},$$
$$\cos k(R_2 - R_1) = \cos(R_2 - R_1)\frac{2\pi}{\lambda}\cdot\operatorname{sign}(\Gamma),$$
$$P_{dir\ trans} = P_T\frac{G_T G_R\lambda^2}{(4\pi R_1)^2},$$
$$P_{ref\ trans} = P_T\frac{G_T G_R\lambda^2}{(4\pi R_2)^2}\cdot|\Gamma|,$$
$$P_{tot} = P_{dir\ trans} + P_{ref\ trans}\cos(R_2 - R_1)\frac{2\pi}{\lambda}\operatorname{sign}|\Gamma|,$$
$$P_{tot\ \mathrm{dBm}} = 10\log_{10}(P_{tot}\cdot 10^{-3})$$

where θ is the incidence angle; R_1, R_2 are the direct and the reflected ray path lengths, respectively; $P_{dir\ trans}$, $P_{ref\ trans}$ are the power quantities of the direct and the reflected waves, respectively; P_{tot}, $P_{tot\ \mathrm{dBm}}$ are the total received

Table 2

The complex permittivity values of typical building materials [7]

Material	η	
	1.0 GHz	57.5 GHz
Concrete	$7.00 - j0.85$	$6.50 - j0.43$
Lightweight concrete	$2.0 - j0.5$	–
Floorboard (synthetic resin)	–	$3.91 - j0.33$
Plaster board	–	$2.25 - j0.03$
Ceiling board (rock wool)	$1.20 - j0.01$	$1.59 - j0.01$
Glass	$7.0 - j0.1$	$6.81 - j0.17$
Fibreglass	$1.2 - j0.1$	–

power quantities in watts and in decibels above one milliwatt.

It follows from Eqs. (6) and (7) given for R_{max} and R_{min}, that the smaller is the angle θ the farther from the geometrical point of reflection is the center of the Fresnel's zone, and the ellipse itself is longer and narrower. At a long distance the lowest, i.e., the first ($n = 1$) lobe of the radiation pattern is the most important. If the angle θ is equal to the angle of the 'axis' of this lobe then the lobe is closer to the ground. For the field at the receiving antenna to be consistent with the interference approach it is necessary for the reflecting ground surface to be smooth (with small disturbances) at least within the first Fresnel's zone. The disturbances outside the first Fresnel's zone have little influence. In optics [8] the disturbances (the deviations from a perfectly flat surface) of the surface of a reflecting mirror must not exceed λ/10 or even λ/16. These values correspond to the normal incidence and can be considered as limiting values. If the incidence is not normal then the influence of disturbances is decreased by a factor of sinθ, allowing for disturbance height

$$\Delta h \le \lambda/(10\sin\theta).$$

For a long radio link the Rayleigh criterion is often used that states that the maximum disturbance height for mirror like reflection is limited by [9]

$$\Delta h \le \lambda/(8\sin\theta).$$

In any practical situation the allowed

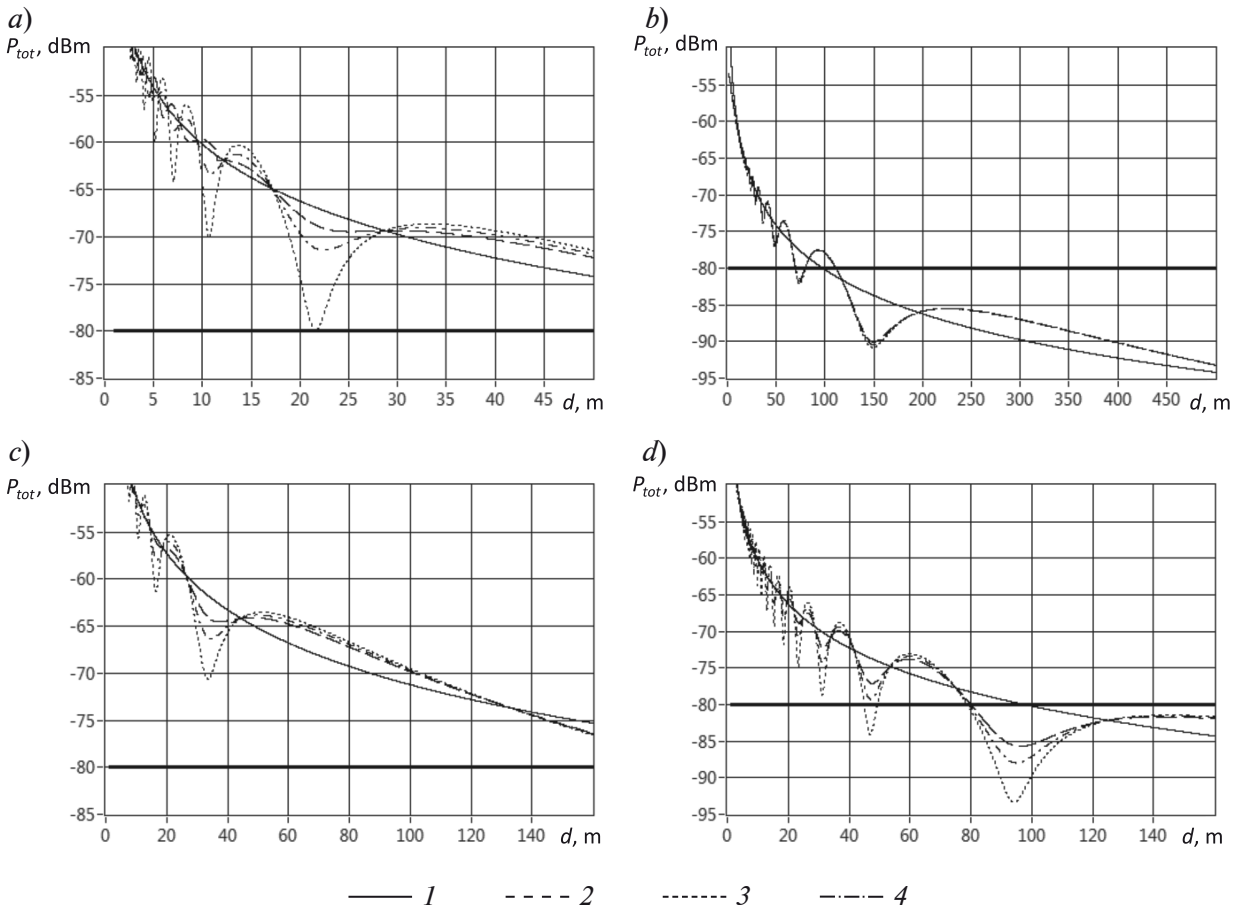

Fig. 2. Plots of the total received radiowave power versus the distance between the 2 antennas of various heights for 2 light sources and various media.

The data was obtained for an ideal link (the Friis equation) (curves *1*) and for a dipole with the vertical (*2*), horizontal (*3*) and circular (*4*) polarizations. The data for EDCLLS (*a*, *b*, *d*) and SPLLS (*c*) light sources is presented; h_1 = 1.15 m (*a*), 1.50 m (*b*), 2.40 m (*c*, *d*); h_2 = 1.15 m (*a*), 6,00 m (*b*), 2.40 m (*c*, *d*); η = 18 − *j*18 (*a*), 12.0 − *j*0.1 (*b*), 7.00 − *j*0.85 (*c*, *d*); P_T = 0 dBm

disturbance height will depend on R_{max1} and $\sin\theta_{max1}$.

For the EDLLS light source discussed above, $\lambda = 0.1227$ m, $\theta_{max1} = 2.18°$ and $\Delta h \leq 0.32$ m. This is in good agreement with another estimate of Δh, according to which the first lobe is properly formed near the maximum at large values of $R \approx d$: $\Delta h \leq h/4$. If $h = 1.5$ m then $\Delta h \leq 0.38$ m.

The results of the radio control link simulation

The received power values in decibels above one milliwatt calculated using the Friis transmission equation and also the radio control link simulation for the vertical, horizontal and circular polarizations are shown in Fig. 2. The plots are created using a software application developed in LabVIEW for simulation of a light source command radio control link taking its specific requirements into account. The program allows calculating the total received power, the reflection coefficients and other parameters of radio wave's propagation as functions of the operating frequency, the heights of a transmitting and a receiving antennas, real and imaginary parts of the dielectric permittivity, the radiation patterns and the transmitter power. A convenient graphical user interface allows studying the results over the wide range of the input parameters. The simulation results help in determining the radio control link range for different mutual orientations (polarizations) of the transmitting and the receiving antennas.

For a horizontal dipole with no directivity in the vertical plane the effect of the ground, reflecting the incident wave towards the receiving antenna, is very strong. It results in the interference of the waves at the receiving antenna which produces a multi-lobed field structure in the equatorial plane of the dipole. The minima and maxima appear at certain values of angle θ in accordance with the above equations. The number of minima is

$$N \geq 2h_1/\lambda + 0.5,$$

where N is the integer number.

Each change in the dipole height by $\lambda/2$ changes the lobe number by one. An increase in h also increases the paths length difference $(R_2 - R_1)$ and places the lobes of the radiation pattern closer to the ground. At the same time $\sin\theta_{max}$ decreases and low objects ($\theta < \theta_{max}$) receive stronger field. An increase in h_2 first improves the reception ($\theta < \theta_{max1}$), then worsens it, then again improves it, etc.

The positions of the maxima and minima of the electric field are determined by the radio control link's geometry and are practically independent of ε_r. However, the more is ε_r value the sharper are the minima and maxima. With a decrease in ε_r the maxima become lower and minima higher, and the multi-lobe structure becomes less prominent. This smoothing tendency grows with decreasing h_1 as long as the multi-lobe structure of the radiation pattern exists, i.e., as long as $h_1, h_2 > \lambda$.

Table 3 shows the total received power $P_{tot\,\mathrm{dBm}}$ for an ideal link (according to the Friis transmission equation) and for a dipole with the vertical (V), circular (C) and horizontal (H) polarizations.

If the ratio h/λ is changed then the lines

Table 3

Calculation results for the total received power (developed in LabVIEW)

Ideal or real link	$P_{tot\,\mathrm{dBm}}$, dBm					
	$\eta = 7.00 - j0.85$		$\eta = 2.00 - j0.85$		$\eta = 1.20 - j0.10$	
	SPLLS	EDCLLS	SPLLS	EDCLLS	SPLLS	EDCLLS
Friis equation	−61.9	−76.0	−61.9	−76.0	−61.9	−76.0
V-dipole	−64.2	−81.0	−65.5	−82.0	−64.9	−81.0
C-dipole	−66.5	−82.6	−66.5	−82.6	−66.0	−81.5
H-dipole	−71.9	−87.8	−67.6	−84.9	−65.1	−82.2

Notes. The input parameters for the SPLLS light source: $f = 868.7$ MHz, $h_1 = h_2 = 2.4$ m, $R_{min1} = 33.33$ m; for the EDCLLS light source: $f = 2445.0$ MHz, $h_1 = 1.5$ m, $h_2 = 2.4$ m, $R_{min1} = 58.68$ m.

limiting the field's variation would remain as before while the $P_{tot\,\max}$ and $P_{tot\,\min}$ values lying on these curves, would move down (in the case of increasing h/λ) towards the smaller θ (and vice versa). The general shape of the curves remains the same. The interference factor Δ, that is equal to the difference

$$\Delta = P_{tot\ for\ V.C.H\text{-}dipol} - P_{tot\,\mathrm{F}}$$

between the real (i.e., $P_{tot\ for\ V.C.H\text{-}dipol}$) and the ideal ($P_{tot\,\mathrm{F}}$) cases, is the largest for a dipole with the horizontal polarization. For the vertical and circular polarizations Δ is practically the same.

The plots of the total received power distribution versus the distance d show that the paths' length difference cannot be small as compared to the wavelength λ for closely spaced antennas. For the horizontal polarization (H-dipole) in the region of oscillations the envelope of the maxima behaves like $\sim 1/R^2$ and the amplitudes of maxima and minima are proportional to the factors $(1+|\Gamma_h|)^2$ and $(1-|\Gamma_h|)^2$ respectively [6]. The last field maximum corresponds to the values of h_1 and h_2 at which $\theta = \theta_{\max 1}$. Starting with the distance where the powers of an ideal and real links become equal the cosine decreases monotonously and the area in which P_{tot} changes with distance like $\sim 1/R^4$ begins. For a long link when $\theta \to 0$ we get the Vvedenskiy transmission equation [8]. For a vertical polarization (V-dipole), the amplitudes of maxima and minima are proportional to the factors

$$[(1+|\Gamma_h|)\cos^2\theta]^2$$

and

$$[(1-|\Gamma_h|)\cos^2\theta]^2$$

limiting the field variations, in the region of oscillations.

If the angle θ is equal to the Brewster's angle θ_0, $(\mathrm{ctg}\theta_0 = \sqrt{\varepsilon})$, the two curves coincide. When vertically polarized waves fall on the surface of an ideal dielectric ($\sigma = 0$, Γ_v is real) at this angle, the reflection coefficient $|\Gamma_h| \to 0$, and its phase is equal to π and $\theta < \theta_0$, and is equal to zero at $\theta > \theta_0$. The difference between H- and V-dipoles described above explains significantly less amplitudes of oscillations in the case of V-dipole.

For very long radio control links, the ratio of the received and the transmitted power is given by the Vvedenskiy transmission equation

$$\frac{P_R}{P_T} = \left(\frac{h_1 h_2}{R^2}\right)^2 \qquad (10)$$

and is independent of polarization and the dielectric permittivity [8].

If $R \approx d$ is small compared to R_2 then $P_{dir\ trans} >> P_{ref\ trans}$, and the limits of a change in the interference factor are significantly reduced. With further decrease of R, the field of the reflected wave can be neglected. In this case the interference factor is close to unity and the Friis transmission equation can be used. It is important to note that all equations derived for an electrically small dipole are applicable to a half-wavelength dipole [8].

The radio control link's range is determined by an equality of the total received power and the receiver sensitivity. In Fig. 2, the radio link's range complies with the first (from the origin) intersection of the receiver sensitivity corresponding to horizontal lines (in decibels above one milliwatt) and the received power depending on the distance. Fig. 2 shows a case when the respective receiver sensitivity is of -80 dBm. For a long unobstructed path (line-of-sight link), the first Fresnel zone breakpoint may occur. The Fig. 2 shows that communication would be lost (in the case of the receiver's sensitivity being of -80 dBm), as a rule, at about the distance $R_{\min 1} = 21$ m for the H-dipole in the minimum of the first Fresnel's zone, while it is obvious that the potential range is longer. For the C- and V-dipoles, a decrease in the signal strength due to diffraction is significantly smaller. If the value of the dielectric permittivity is about 1 to 2 then a decrease in the signal strength is again significantly smaller and is practically the same for any polarization.

According to the recommendations given in Ref. [7], in the line-of-sight channels, directional C-polarization antennas offer an effective means of reducing the delay spread. When the C-polarization signal is incident on a reflecting surface at an incidence angle larger than the Brewster's one, the handedness of the reflected C-polarization signal is reversed. The reversal of the C-polarization signal at each reflection means that multipath components arriving after one reflection are orthogonally

polarized to the line-of-sight component and this eliminates a significant proportion of the multipath interference. Since all existing building materials exhibit Brewster angle less than 45° ($\varepsilon_r = 7.0, 2.0, 1.2 \leftrightarrow \theta_0 = 8.13°, 26.15°, 39.80°$) multipath propagation due to a single reflection (that is the main source of multipath components) is effectively suppressed in most environments irrespective of the interior structure and materials in the room.

Summary

Light emitting diode lighting technologies drastically change the possibilities of control of the light quality. Smart light can be created by changing spectral content, color and intensity of lighting in time. Energy efficient dynamically controlled light sources find application in lighting systems of medical institutions, in museums and art exhibitions providing the best color reproduction of paintings, in industrial lighting for improving working conditions and increasing attentiveness of personnel. This paper discusses two variants of design and construction of wireless networks of dynamically controlled polychromatic light sources: using ISM/SRD and ZigBee (IEEE 802.15.4) technologies. Optical lighting modules are built using AlInGaN and AlGaInP structures, have a luminous efficiency of 85 – 120 lm/W and varying light temperatures from relaxing (T_c = 1700 K) to activating (T_c = 10000 K). Such controlled LED light sources can be used to correct the psychophysiological state of people.

The maximally continuous spectrum approaching the natural light is achieved providing the high values of color rendering indexes as well as their leveling. A hardware-software complex supporting testing, tuning and control of a network in various modes of operation is developed.

The most convenient dynamic control method for LED light sources is the use of a radio control link. The received power may be computed using the two-ray model: a line-of-sight ray and a reflected one. This approach is significantly different (it is much simpler) as compared to cellular networks in which multiple reflections from various objects results in the multi-path propagation. A software application was developed in LabVIEW for link simulation that has a convenient user interface for setting the parameters of a radio control link with horizontal, vertical and circular polarizations. The circular polarization is most effective in the case of the multi-path propagation in the operating area of energy efficient dynamically controlled LED light sources.

REFERENCES

[1] **P.R. Boyce,** The impact of light in buildings on human health, Indoor and Built Environment. 19 (1) (2010) 8–20.

[2] **D.Y. Su, C.C. Liu, C.M. Chiang, W. Wang,** Analysis of the long-term effect of office lighting environment on human reponses, International Journal of Social, Behavioral, Educational, Economic, Business and Industrial Engineering. 6 (7) (2012) P. 2.

[3] **A.V. Aladov, V.N. Aladov, V.P. Valyukhov, et. al.,** Type LED dynamically controlled light sources for novel lighting technology, St. Petersburg Polytechnical University Journal. Physics and Mathematics. (4) (2014) 38–47.

[4] **D. Gislason,** Zigbee wireless networking, San Juan Software, Friday Harbor, WA, United States (2008).

[5] **A.V. Aladov, V.P. Valyukhov, S.V. Demin, et al.,** Wireless network of controlled energy-efficient LED lighting source, St. Petersburg Polytechnical University Journal. Physics and Mathematics. (1) (2015) 29–36.

[6] **T.I. Kvaksrud,** Range measurements in an open field environment, Design Note DN018. Texas Instruments, SWRA 169A, 1–14.

[7] Recommendation ITU-RP. P.1238-2. Propagation data and prediction methods for the planning of indoor radio communication systems and radio local area networks in the frequency range 900 MHz to 100 GHz// www. itu.int/rec/R-REC. P.1238/en

[8] **B.A. Vvedenskiy, A.G. Arenberg,** On propagation of ultrashort radiowaves, Moscow, Soviet Radio (1948).

[9] **G.T. Markov, B.M. Petrov, G.P. Grudinskaya,** Electrodynamics and radiowave propagation, Moscow, Soviet Radio (1979).

Received 21.12.16, accepted 09.02.2017.

THE AUTHORS

ALADOV Andrey V.
Submicron Heterostructures for Microelectronics Research and Engineering Center of the RAS
26 Politekhnicheskaya St., St. Petersburg, 194021, Russian Federation
aaladov@mail.ioffe.ru

VALYUKHOV Vladimir P.
Peter the Great St. Petersburg Polytechnic University
29 Politechnicheskaya St., St. Petersburg, 195251, Russian Federation
Valyukhov@yandex.ru

KUPTSOV Vladimir D.
Peter the Great St. Petersburg Polytechnic University
29 Politechnicheskaya St., St. Petersburg, 195251, Russian Federation
vdkuptsov@yandex.ru

DEMIN Sergey V.
Submicron Heterostructures for Microelectronics Research and Engineering Center of the RAS
26 Politekhnicheskaya St., St. Petersburg, 194021, Russian Federation
demin@mail.ioffe.ru

VALYUKHOVA Anna V.
Peter the Great St. Petersburg Polytechnic University
29 Politechnicheskaya St., St. Petersburg, 195251, Russian Federation
avalyukhova@imop.ru

СПИСОК ЛИТЕРАТУРЫ

1. **Boyce P.R.** The impact of light in buildings on human health // Indoor and Built Environment. 2010. Vol. 19. No. 1. Pp. 8–20.

2. **Su D.Y., Liu C.C., Chiang C.M., Wang W.** Analysis of the long-term effect of office lighting environment on human responses // International Journal of Social, Behavioral, Educational, Economic, Business and Industrial Engineering. 2012. Vol. 6. No. 7. P. 2.

3. **Аладов А.В., Аладов В.Н., Валюхов В.П., Закгейм А.Л., Цацульников А.Ф.** Динамически управляемые светодиодные источники света для новых технологий освещения // Научно-технические ведомости СПбГПУ. Физико-математические науки. 2014. № 4(206). С. 38 – 47.

4. **Gislason D.** Zigbee wireless networking. WA. United States: San Juan Software, Friday Harbor, 2008. 425 p.

5. **Аладов А.В., Валюхов В.П., Демин С.В., Закгейм А.Л., Цацульников А.Ф.** Беспроводная сеть управляемых энергоэффективных светодиодных источников освещения // Научно-технические ведомости СПбГПУ. Физико-математические науки. 2015. № 1(213). С. 50 – 60.

6. **Kvaksrud T.I.** Range measurements in an open field environment// Design Note DN018. Texas Instruments. SWRA 169A. Pp. 1–14.

7. Recommendation ITU-RP. P.1238-2. Propagation data and prediction methods for the planning of indoor radio communication systems and radio local area networks in the frequency range 900 MHz to 100 GHz // www. itu.int/rec/R-REC. P.1238/en

8. **Введенский Б.А., Аренберг А.Г.** Вопросы распространения ультракоротких волн. М.: Советское радио, 1948. 144 с.

9. **Марков Г.Т., Б.М. Петров, Г.П. Грудинская.** Электродинамика и распространение радиоволн. М.: Советское радио, 1979. 374 с.

Статья поступила в редакцию 21.12.2016, принята к публикации 09.02.2017.

СВЕДЕНИЯ ОБ АВТОРАХ

АЛАДОВ Андрей Вальменович – *кандидат физико-математических наук, старший научный сотрудник Научно-технологического центра микроэлектроники и субмикронных гетероструктур РАН, Санкт-Петербург, Российская Федерация.*

194021, Российская Федерация, Санкт-Петербург, Политехническая ул., 26
aaladov@mail.ioffe.ru

ВАЛЮХОВ Владимир Петрович – *доктор технических наук, профессор кафедры радиофизики Санкт-Петербургского политехнического университета Петра Великого, Санкт-Петербург, Российская Федерация.*
195251, Российская Федерация, Санкт-Петербург, Политехническая ул., 29
valyukhov@yandex.ru

КУПЦОВ Владимир Дмитриевич – *кандидат технических наук, доцент кафедры радиофизики Санкт-Петербургского политехнического университета Петра Великого, Санкт-Петербург, Российская Федерация.*
195251, Российская Федерация, Санкт-Петербург, Политехническая ул., 29
vdkuptsov@yandex.ru

ДЕМИН Сергей Васильевич – *заведующий лабораторией Научно-технологического центра микроэлектроники и субмикронных гетероструктур РАН, Санкт-Петербург, Российская Федерация.*
194021, Российская Федерация, Санкт-Петербург, Политехническая ул., 26
demin@mail.ioffe.ru

ВАЛЮХОВА Анна Владимировна – *ассистент высшей школы международных образовательных программ Санкт-Петербургского политехнического университета Петра Великого, Санкт-Петербург, Российская Федерация.*
195251, Российская Федерация, Санкт-Петербург, Политехническая ул., 29
avalyukhova@imop.ru